Raman scattering from vibrational modes in Si_{46} clathrates

S. L. Fang, L. Grigorian, and P. C. Eklund
Department of Physics and Astronomy, University of Kentucky, Lexington, Kentucky 40506-0055

G. Dresselhaus and M. S. Dresselhaus
Massachusetts Institute of Technology, Cambridge, Massachusetts 02139

H. Kawaji and S. Yamanaka
Department of Applied Chemistry, Faculty of Engineering, Hiroshima University, Higashi-Hiroshima 739, Japan

(Received 15 January 1997; revised manuscript received 7 November 1997)

Room-temperature Raman-scattering spectra are reported for the type-II superconductors $M_xBa_ySi_{46}$ (M =Na,K) that were recently shown to exhibit T_c's ~3.5 K. These spectra are compared to those of Na_8Si_{46} and K_7Si_{46} clathrates that exhibit normal metallic behavior down to 2 K. In the Si_{46} system, fifteen of the eighteen Si related first-order Raman frequencies predicted by group theory have been detected, and the frequencies are found to be sensitive to the particular dopants. The Raman linewidths observed for the $M_xBa_ySi_{46}$ system are comparable to those observed for Na_8Si_{46} and K_7Si_{46}. The data, taken collectively, suggest that the line broadening in the metallic Si clathrates is due to important contributions from both the electron-phonon interaction as well as from a random filling of the Si cages and charge-transfer disorder.
[S0163-1829(98)01810-4]

INTRODUCTION

In this paper we report Raman-scattering results on the vibrational modes of Si clathrates. This work was motivated by the recent reports by Yamanaka and co-workers of superconductivity in the $M_xBa_ySi_{46}$ (M=Na, K) compounds that were reported to exhibit superconductivity with a transition temperature T_c ~3.5 K.[1,2] We discuss room-temperature and 10 K Raman spectra obtained on superconducting Si_{46} clathrate samples. The results are compared to those on metallic, but not superconducting, Si_{46} clathrates. So far, little experimental information on the electronic and phonon dynamics of these materials is known, and the effect of doping on the lattice dynamics has also not yet been explored.

The silicon clathrate compounds M_xSi_{46} and M_xSi_{136} (M=Na, K, Rb, and Cs) were first synthesized in 1965 and studied extensively by Hagenmüller and co-workers.[3,4] The crystal structure of these compounds consists of polyhedral Si cages that form around metal atoms during synthesis. Two distinct cages are found in the Si_{46} clathrates. One is a dodecahedron (Si_{20}) with 12 pentagonal faces, and the other is a tetrakaidecahedron (Si_{24}) with 12 pentagonal and 2 opposing hexagonal faces. As shown in Fig. 1, these polyhedra share faces forming a three-dimensional isotropic sp^3 covalent network. As in the diamond Si (fcc lattice), all Si atoms are tetrahedrally coordinated. The structures of the Si clathrates, zeolites,[5] gas hydrates,[6] and endohedral fullerene solids[7] also employ large polyhedra as the basic building blocks. The Si clathrates and gas hydrates are similar to fullerene solids as the polyhedral building blocks exhibit only pentagonal and hexagonal faces. A significant difference between the Si clathrates and fullerene solids is their solid state, intercage bonding. In fullerene solids, the polyhedra are held together by weak van der Waals-type interactions and the physical properties are strongly related to those of the individual cages (or molecules). Nevertheless, the alkali-metal doped C_{60} materials are superconducting, for example, for the stoichiometries M_3C_{60}, M=K (T_c=19.3 K), M=Rb (T_c=29.6 K).[8,9] In the Si clathrates, however, the polyhedra share pentagonal and hexagonal faces and form a covalently bonded lattice. Reasonably broad electronic bands are therefore anticipated. The M_xSi_{46} clathrate compounds are generally found to form metallic ''line'' compounds in which x=8, 7, 5 for Na, K, Rb, respectively.[4] The observed x dependence for these line compound stoichiometries was proposed to be related to the size of the M atoms, but this has never been explained theoretically.[4]

A second family of clathrates, M_xSi_{136}, can also be formed in which x can be varied over a wide range for a particular choice of M. This Si clathrate system has been shown experimentally to be generally metallic for $x>10$, and semiconducting for $x<10$.[4] The structure for the Si_{136} clathrates is similar, but distinct from the Si_{46} clathrates, involving a periodic lattice of Si_{20} and Si_{28} cages.

Recently, the energetics and band structures of the Si

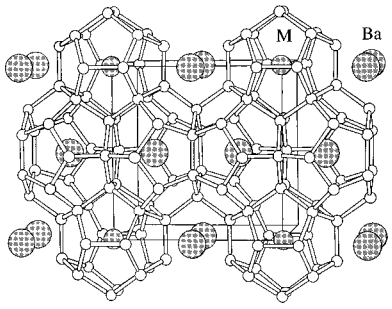

FIG. 1. Simple cubic structure of $M_2Ba_6Si_{46}$. Only the Si polyhedra for the front face are shown.

clathrates (without alkali metals) have been examined.[10] It was predicted that the energy of these ''empty'' structures is only slightly above that of the ground-state diamond structure (by about 0.07 eV/atom). Furthermore, both the empty ($x=0$) Si_{46} and Si_{136} theoretical crystals were found to exhibit an indirect band gap of about 1.9 eV, i.e., about 0.7 eV larger than that of Si in the diamond structure, and comparable to the experimentally observed optical band gap of porous Si (Ref. 11) that is thought to stem from quantum confinement effects. The Si clathrate structures suggest an alternative approach to Si band-gap engineering, and these clathrates may become an important new class of semiconductors.[12]

The effects of doping Si clathrates with alkali metals have also been investigated theoretically.[13] The calculations show that the metal atoms donate electrons to the conduction bands and these doped clathrates are therefore metallic. Furthermore, since the metal atoms are located inside the silicon cages, the Si clathrates are very stable in air and even in acid solutions.[1] Three groups have studied theoretically the structural and vibrational properties of the Si clathrates Si_{136} and Si_{46}, assuming that the cages are empty.[14–16] Their results are discussed below.

Recently, Yamanaka and co-workers reported bulk superconductivity in the Si_{46} clathrates, $Na_{2.9}Ba_{4.5}Si_{46}$ and $K_{2.9}Ba_{4.9}Si_{46}$.[1,2] These materials were reported to be type-II superconductors with a critical temperature $T_c \sim 3.5$ K. Electrical resistivities of Ba-doped clathrates above T_c were found to be almost constant (10–30 mΩ cm) up to room temperature and are of the same order as those found for nonsuperconducting ($T>2$ K) Na_8Si_{46} and K_7Si_{46}.[2,4,17] Soon after this report, Saito and Oshiyama calculated the band structure for the ideal stoichiometry $Na_2Ba_6Si_{46}$ and found a strong hybridization between the Si_{46} band and a barium orbital, resulting in a very high density of states at the Fermi level, $N(\varepsilon_F) \sim 48$ states /eV.[18] This electronic effect was proposed to be important for the superconductivity in the Si_{46} clathrates.[18]

In the conventional Bardeen-Cooper-Schrieffer theory for phonon-mediated superconductivity, the critical temperature for superconductivity (T_c) can be estimated as

$$T_c = 1.13\Theta_D \exp\left(-\frac{1}{\lambda}\right), \tag{1}$$

where Θ_D is the Debye frequency and λ is the electron-phonon coupling constant. Furthermore, λ can be written as the product of $N(\varepsilon_F)$ and V, where $N(\varepsilon_F)$ is the density of electron states at the Fermi level, and V is the average electron pairing interaction. This formula suggests that there are three ways to engineer an increase in the T_c of a material system: to stiffen the lattice and thereby increase the Debye frequency, increase the pairing interaction, or increase $N(\varepsilon_F)$. From this perspective, the report of superconductivity in Si clathrates is interesting, since the Θ_D in this class of solids is expected to be relatively high, and $N(\varepsilon_F)$ has also been shown theoretically to be large for Ba as the dopant. Other dopant elements may also further enhance T_c through an increase in $N(\varepsilon_F)$. The physics of V remains to be elucidated. The motivation of this work is to investigate possible correlations between the Raman-scattering spectra and the superconducting properties of the Si clathrate samples.

EXPERIMENTAL DETAILS

The preparation of Ba-doped Si_{46} clathrates has been described in detail elsewhere.[2,17] Briefly, two Zintl phases of the silicides $BaSi_2$ and MSi (M=Na or K), were mixed stoichiometrically and placed in a Ta tube that was vacuum sealed in a stainless-steel cylinder. The mixture was heated at 600 °C for several days to obtain a third metal silicide Na_2BaSi_4. The silicide was then evacuated at elevated temperature (500 °C) under vacuum. As a result, part of the M atoms were removed, and the Si_{46} clathrate containing M and Ba in the cages is formed. X-ray structural analysis (Rietveld) was performed and the results indicate that Ba atoms occupy the cavities of the larger Si_{24} cages (tetrakaidecahedra) and M atoms reside mainly inside the smaller Si_{20} cages (dodecahedra).[2,17] Some cages could be empty, depending on the conditions of sample preparation. Chemical analysis indicated that the samples used for this work are $Na_{0.2}Ba_{5.6}Si_{46}$ and $K_{2.9}Ba_{4.9}Si_{46}$. Both samples were characterized by x-ray-powder diffraction, electrical resistivity measurements, and temperature-dependent magnetization measurements. The T_c for the two samples studied here are 3.5 K ($Na_{0.2}Ba_{5.6}Si_{46}$) and 3.2 K ($K_{2.9}Ba_{4.9}Si_{46}$). For comparison, we also collected Raman-scattering spectra of semiconducting Na_xSi_{136} and metallic Na_8Si_{46} and K_7Si_{46} samples. These samples were prepared at the University of Kentucky as follows. First, silicon powder was loaded with a large excess of Na (or K) in a sealed stainless-steel ampoule located in vacuum in a sealed quartz tube and heated to 600 °C. This resulted in the formation of the compound NaSi (KSi) and excess elemental Na (K). This mixture was heated under $\sim 10^{-3}$ Torr dynamic vacuum at about 330 °C for a period of several days, decomposing the silicides and yielding Si_{46} or Si_{136}, depending on the decomposition temperature. Rietveld analysis showed that the polycrystalline powders exhibited structures consistent with those reported by Kasper *et al.*[3] A small amount of diamond-phase (fcc) Si was also found to be present in the Na_8Si_{46} sample.

We have measured the dc magnetic susceptibility $\chi(T)$ of Na_8Si_{46} and K_7Si_{46} samples in an external magnetic field of 10 Oe with a Quantum Design MPMS superconducting quantum interference device magnetometer. No diamagnetic signal indicative of superconductivity was observed down to 2 K (the lowest attainable temperature). As far as we know, this observation is the first direct measurement of $\chi(T)$ for essentially single-phase Na_8Si_{46} and K_7Si_{46} samples in search of superconductivity. Earlier, magnetic susceptibility measurements with a Faraday balance had been carried out with mixed-phase samples of the Na_xSi_{136} phase ($2<x<19$), diamond-phase Si, and a significant (unspecified) amount of Na_8Si_{46} phase, and their $\chi(T)$ results also showed no evidence for superconductivity down to 2 K.[19]

Raman-scattering experiments were carried out in the Brewster backscattering geometry on characterized pelletized powders using the 5145 Å line of an argon-ion laser. Using a mortar and pestle, the Si clathrate powders were mixed with 20 wt % KBr and then pressed into small pellets. A cylindrical lens was employed to create an illuminated

TABLE I. Crystallographic description for $M_2Ba_6Si_{46}$ based on Rietveld refinement.

Space Group $Pm3n$ (O_h)			
Atomic position	x	y	z
6 Si in 6 (c)	$\frac{1}{4}$	0	$\frac{1}{2}$
16 Si in 16 (i)	a	a	a
24 Si in 24 (k)	0	b	c
2 M in 2 (a)	0	0	0
6 Ba in 6 (d)	$\frac{1}{4}$	$\frac{1}{2}$	0

stripe ($0.1\times 2\ mm^2$) on the sample surface. Low laser flux ($20\ mW/mm^2$) was used in order to prevent damage to the samples. A 0.46 m, $f/5$ single grating spectrometer (Jobin-Yvon HR460) equipped with a charge-coupled-device detector cooled by liquid nitrogen was used to collect the Raman spectra. The system spectral resolution is about $2\ cm^{-1}$. Polarization analysis of the scattered light was carried out using a polaroid sheet and a subsequent polarization scrambler to remove instrument polarization effects.

RESULTS AND DISCUSSION

The Si_{46} lattice (Fig. 1) is a simple cubic (sc) lattice with a space group symmetry $Pm3n$.[1] In the figure, the specific structure is for $M_2Ba_6Si_{46}$, where the Ba atoms (or presumably Ba^{2+} ions) occupy the larger Si_{24} cages.[1] For clarity, only the atoms associated with cages located on one face of the primitive cell are shown. The structure of the Si_{46} clathrate may be explained by arranging the polyhedra in the following way. A Si_{20} dodecahedron is centered at each sc lattice point and all eight dodecahedra in the unit cell are oriented in the same way. A second dodecahedron, rotated 90° relative to the first, is placed at the body center of the cube. To make the solid fully fourfold coordinated, six additional atoms are present in the unit cell. They generate six Si_{24} tetrakaidecahedra that fill the space not occupied by the dodecahedra. A crystallographic description for the $M_2Ba_6Si_{46}$ clathrates is given in Table I. There are three inequivalent atomic sites in the $Pm3n$ structure for the silicon atoms: 6 Si atoms @ 6 (c), 16 Si atoms @ 16 (i), and 24 Si atoms @ 24 (k). The corresponding site symmetries for the three silicon sites are D_{2d}, C_3, and C_s, respectively.[20] The barium atoms occupy the 6 (d) site with D_{2d} symmetry, which is at the center of the Si_{24} tetrakaidecahedron. The alkali-metal M atoms occupy the 2 (a) sites with T_h symmetry that are located at the center of the Si_{20} dodecahedra. Based on this symmetry information, group theoretical analysis for the *ideal composition* $M_2Ba_6Si_{46}$ was carried out. The results of the group theoretical analysis for the IR-allowed and Raman-allowed vibrational modes are shown in Table II, where the ungerade (u) and gerade (g) modes are IR and Raman active, respectively.[21]

For a formula unit of $M_2Ba_6Si_{46}$ there are 3 (54 atoms) $=172$ degrees of freedom. In a first-order (one-phonon) process only 13 T_{1u} (3) modes are IR active, where the (3) indicates that these $q=0$ T_{1u} phonon modes are triply degenerate (q is the phonon wave vector). In addition to the one triply degenerate T_{1u} acoustic ($\omega\approx 0$) mode, there are 12 other T_{1u} IR-active optical phonons. The first-order Raman-active modes are determined by group theory to have $3A_{1g}(1)+8E_g(2)+9T_{2g}(3)$ symmetries. Based on group theoretical arguments, the A_{1g} modes should be polarized, and the E_g and T_{2g} modes should be unpolarized in isotropic well-ordered samples, i.e., samples that are unoriented, polycrystalline grains exhibiting good crystallographic order. One of the $8E_g$ modes is associated with Ba displacements and would be expected to have a low frequency. The $9T_{2g}$ modes have one mode at very low frequency associated with Ba displacements and 8 modes associated with Si displacements that should be found at much higher frequencies, relatively. The remaining degrees of freedom are associated with silent optical phonons that are neither Raman nor IR active at $q=0$.

The room-temperature Raman spectra for the 3.5 K superconductors $Na_{0.2}Ba_{5.6}Si_{46}$ and $K_{2.9}Ba_{4.9}Si_{46}$, and for the metallic Na_8Si_{46} and K_7Si_{46} are shown in Figs. 2(a) and 2(b), respectively. The results of a Lorentzian lineshape analysis are also shown. The data are represented by the points and the solid line is the fit to the spectrum. Individual Lorentzians are shown below the experimental spectrum. In all cases, a smooth polynomial background has been subtracted from the data for clarity. Since some of the modes are unresolved in the spectra of $Na_{0.2}Ba_{5.6}Si_{46}$ and $K_{2.9}Ba_{4.9}Si_{46}$, we have fitted these spectra in a manner consistent with the results obtained for Na_8Si_{46} where the Raman bands are better resolved. Furthermore, it should be emphasized that the Ba-doped samples exhibited superconductivity below $\sim$3.5 K. Note that the Raman band positions and widths in Figs. 2(a) and 2(b) are sensitive to the particular alkali-metal dopant (i.e., Na and K). Twenty Raman frequencies are predicted by group theory and eighteen of them are associated with Si displacements. We have observed 12 distinct Raman bands for $Na_{0.2}Ba_{5.6}Si_{46}$, 13 for $K_{2.9}Ba_{4.9}Si_{46}$, 15 for Na_8Si_{46}, and 15 for K_7Si_{46} at room temperature. Since the eighteen Si modes should be found at relatively higher frequencies, we assume that the modes observed here are related to Si. These Raman bands are somewhat broad. In some cases, these

TABLE II. Vibrational irreducible representations for $M_2Ba_6Si_{46}$.

No. of atoms	Designation	Irreducible representations
2 M	a	$T_{1u}+T_{2u}$
6 Ba	d	$A_{2g}+E_g+T_{1g}+T_{2g}+2T_{1u}+T_{2u}$
6 Si	c	$A_{2g}+E_g+T_{1g}+T_{2g}+2T_{1u}+T_{2u}$
16 Si	i	$A_{2g}+A_{2g}+2E_g+3T_{1g}+3T_{2g}+A_{2u}+A_{2u}+2E_u+3T_{1u}+3T_{2u}$
24 Si	k	$2A_{2g}+2A_{2g}+4E_g+4T_{1g}+4T_{2g}+A_{2u}+A_{2u}+2E_u+5T_{1u}+5T_{2u}$

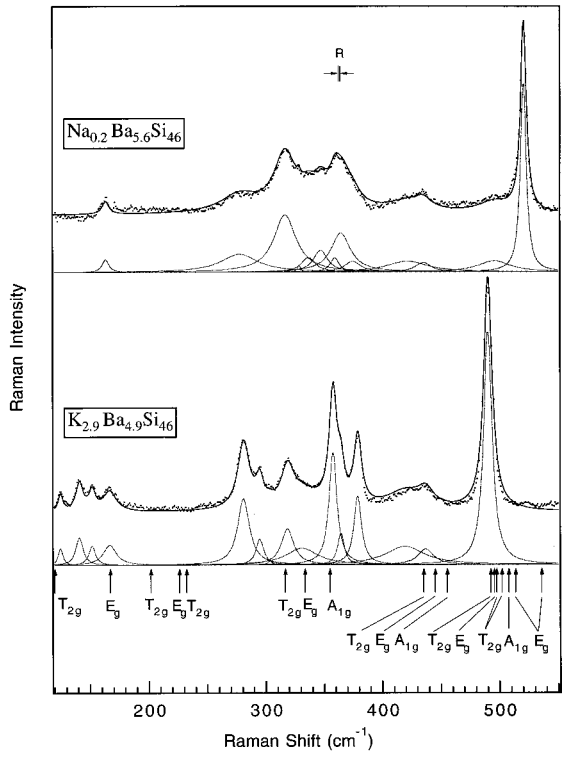

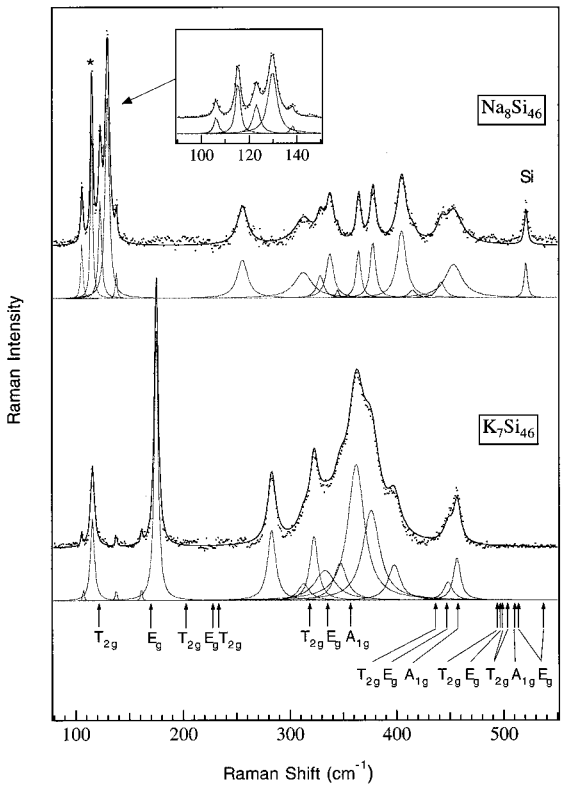

FIG. 2. (a) Raman spectra of $Na_{0.2}Ba_{5.6}Si_{46}$ and $K_{2.9}Ba_{4.9}Si_{46}$ at $T=300$ K. The data are represented by the points and the solid lines are the fit to the spectrum. The arrows indicate the Raman frequencies calculated by Alben *et al.* (Ref. 15). The ''*R*'' indicates the resolution of the system. (b) Raman spectra of Na_8Si_{46} and K_7Si_{46} at $T=300$ K. The data are represented by the points and the solid lines are the fit to the spectrum. The arrows indicate the Raman frequencies calculated by Alben *et al.* The peak marked with a * is an artifact identified with a plasma line from the Ar ion laser.

broad bands may contain unresolved Raman lines. The strongest bands in the spectra of the two superconducting samples appear close in frequency ($\sim 500-520\ cm^{-1}$) to strong lines observed in possible minority phases, i.e., silicides and Si in the diamond structure. For example, in the $Ca_{1-x}La_xSi_2$ silicides, a strong Raman line has been reported in the range of $510-515\ cm^{-1}$, exhibiting a weak x dependence,[22] and in silicon (diamond structure) a single, Raman-allowed line is found at $520\ cm^{-1}$. Therefore, the assignment for the strong band at $500.0\ cm^{-1}$ for $K_{2.9}Ba_{4.9}Si_{46}$ as well as the strong band at $520.5\ cm^{-1}$ for $Na_{0.2}Ba_{5.6}Si_{46}$ to a Si clathrate mode(s) is not made in this work. In support of this view is the absence of any bands in the range $500-550\ cm^{-1}$ in the Na_8Si_{46} and K_7Si_{46} spectra [Fig. 2(b)]. Consistent with the x-ray data, the weak band at $520\ cm^{-1}$ in Na_8Si_{46} is assigned to a small amount of Si (diamond structure) in the sample. It is also interesting to note that no bands near $520\ cm^{-1}$ are detected in the Raman spectra of semiconducting Na_3Si_{136}.[23]

Group theory indicates that for the incident electric field (E) in the plane of incidence (II), the A_{1g} modes should only be observable in the (II, II) polarization geometry when both the incident and scattered electric vectors are parallel to the plane of incidence. However, our polarization measurements show that none of the observed Raman modes are strongly polarized. Three possible reasons can be proposed: (1) the A_{1g} modes are relatively weak and not observed at all, (2) the A_{1g} modes are very much broadened by electron-phonon interaction and thus are not observable, (3) the Raman polarization selection rules for the A_{1g} modes are relaxed because of Ba and/or (Na, K) doping disorder. The latter, we feel, is the more likely explanation, as A_{1g} modes tend to be the most intense modes for many solids. Raman scattering may thus be much more sensitive than x-ray-powder diffraction to random cage filling in the clathrates.

The results of a Lorentzian lineshape analysis (frequency and linewidth) for the Raman spectra of the Si clathrates shown in Figs. 2(a) and 2(b) are listed in Table III. The similarity among the four spectra should be noted, especially in the region of $250-480\ cm^{-1}$. We have attempted to correlate the modes observed in these four Si_{46} compounds in Table III. As mentioned earlier, three groups have calculated the $q=0$ Raman frequencies of the Si_{46} clathrate structure with *empty* cages, i.e., the ''undoped'' lattice.[14–16] Only Menon and co-workers[16] performed the calculations on the optimized (i.e., ''relaxed'') structures. They used a generalized tight-binding molecular dynamics method. The other two calculations were for unrelaxed structures. Alben *et al.* used the semiempirical force-constant scheme,[15] and Kahn and Lu used the O(N) tight-binding density-matrix approach.[14] They all find 18 Raman-active and 10 infrared-active modes, which have $3A_{1g}(1)+7E_g(2)+8T_{2g}(3)+10T_{1u}$ symmetries. However, their calculated frequencies do not agree very well with each other, or with the data as can be seen in Tables III and IV. Since we observe very noticeable, dopant-dependent changes in the Raman frequencies of these superconducting and metallic clathrates, it is clear that the empty lattice model needs improvement. A more sophisticated theory, including structural relaxation, charge transfer between the dopant (M) and the Si cages, and Si-M interactions appear to be necessary to quantitatively understand our data.

TABLE III. Raman mode frequencies (ω) and widths (Γ) for superconducting $Na_{0.2}Ba_{5.6}Si_{46}$ and $K_{2.9}Ba_{4.9}Si_{46}$, and metallic Na_8Si_{46} and K_7Si_{46}. Modes appear in the same row are considered to be related.

$Na_{0.2}Ba_{5.6}Si_{46}$		$K_{2.9}Ba_{4.9}Si_{46}$		$K_{2.9}Ba_{4.9}Si_{46}$[a]		Na_8Si_{46}		K_7Si_{46}	
ω (cm^{-1})	Γ (cm^{-1})	ω (cm^{-1})	Γ (cm^{-1})	ω (cm^{-1})	Γ (cm^{-1})	ω (cm^{-1})	Γ (cm^{-1})	ω (cm^{-1})	Γ (cm^{-1})
						106.2	3.2	105.6	3.2
		125.0	5.0	128.7	3.1	123.1	4.2	115.8	4.3
						129.8	4.4		
						138.1	3.1	137.8	3.0
		141.0	7.3	144.6	3.5				
		151.7	6.7	157.7	3.2			161.3	3.1
163.5	6.8	166.7	13.4	174.3	5.4			175.2	4.2
277.9	38.9					255.9	11.8		
316.9	23.0	281.0	12.1	280.7	8.7	313.1	20.2	283.1	9.0
328.8	4.5	295.0	7.8	296.3	4.0	328.9	7.7	313.2	12.7
347.4	14.6					338.1	8.2	322.8	9.1
336.9	14.3	318.6	12.9	324.4	5.9	345.2	4.5	333.1	23.5
359.6	9.0	331.1	33.0			364.9	5.2	347.6	14.4
364.8	20.1	357.7	8.1	360.3	5.2	378.4	6.2	362.5	18.4
374.9	16.2	364.5	6.7	367.7	4.4	405.3	10.1	376.5	19.1
		378.9	7.9	382.9	5.1	415.6	8.2	398.2	13.7
421.6	41.1	419.3	39.6	425.2	38.9	442.1	8.7	448.5	10.1
435.3	15.9	437.0	16.0	447.9	16.9	453.8	19.2	456.8	7.9
495.8	32.8								

[a]All data for $T = 300$ K except for the $K_{2.9}Ba_{4.9}Si_{46}$ data identified with a (*) for $T = 10$ K.

As can be seen in Fig. 2(a) the two $T = 300$ K spectra for the superconducting clathrates are quite similar, albeit the Raman lines in the $Na_{0.2}Ba_{5.6}Si_{46}$ spectrum are, in many cases, noticeably up-shifted relative to their spectral counterparts in $K_{2.9}Ba_{4.9}Si_{46}$. The shift is not rigid for every mode, as shown in Table III. The question is whether or not this shift, or the broader linewidths observed in the $Na_{0.2}Ba_{5.6}Si_{46}$ clathrate, tell us anything about the superconducting pairing mechanism, as discussed below.

Since the T_c's for both of the $Na_{0.2}Ba_{5.6}Si_{46}$ and

TABLE IV. The calculated Raman-active mode frequencies (in units of cm^{-1}) and associated irreducible representations for empty Si_{46} at the zone center, by Kahn and Lu, Alben *et al.*, and Menon and co-workers.

Kahn and Lu (Ref. 14)		Alben *et al.* (Ref. 15)		Menon and co-workers (Ref. 16)	
Energy	Mode	Energy	Mode	Energy	Mode
595.8	E_g	536	E_g	508	E_g
592.5	A_{1g}	513	E_g	492	A_{1g}
591.8	T_{2g}	509	A_{1g}	492	T_{2g}
588.3	T_{2g}	502	T_{2g}	489	E_g
582.5	E_g	497	T_{2g}	485	T_{2g}
578.2	T_{2g}	496	E_g	477	T_{2g}
563.7	E_g	493	T_{2g}	471	E_g
512.2	A_{1g}	455	A_{1g}	431	A_{1g}
501.3	T_{2g}	444	E_g	418	E_g
499.9	E_g	435	T_{2g}	415	T_{2g}
392.0	A_{1g}	355	A_{1g}	328	A_{1g}
348.3	E_g	332	E_g	297	E_g
347.5	T_{2g}	317	T_{2g}	291	T_{2g}
241.7	E_g	231	T_{2g}	212	E_g
167.0	T_{2g}	226	E_g	184	T_{2g}
161.3	T_{2g}	201	T_{2g}	170	T_{2g}
143.3	E_g	168	E_g	141	E_g
109.8	T_{2g}	120	T_{2g}	106	T_{2g}

$K_{2.9}Ba_{4.9}Si_{46}$ are essentially equal (~3.5 K) and Raman spectra similar to these materials are also observed for Na_8Si_{46} and K_7Si_{46} [Fig. 2(b)], it seems unlikely that the difference in Raman *frequencies* observed is due to the electron-phonon interaction (i.e., frequency renormalization). The doping-dependent differences observed for the Raman bands in $Na_{0.2}Ba_{5.6}Si_{46}$ and their counterparts in $K_{2.9}Ba_{4.9}Si_{46}$ [Fig. 2(a)] may be due to several other factors. First, the Si-*M* interaction may be responsible, as the mass of K is almost a factor of two larger than Na. Second, there is a doping dependence of the Si-Si bondlengths as evidenced in the lattice constant.[17] X-ray-diffraction data reveal that the lattice constant for $K_{2.9}Ba_{4.9}Si_{46}$ (10.273 Å) is slightly larger than that of $Na_{0.2}Ba_{5.6}Si_{46}$ (10.261 Å), consistent with the larger *M* atom (ion) size.[1,2] This lattice expansion should weaken the Si-Si bonds, consistent with the observed red shift in the Raman spectrum of the K-doped sample relative to that of the Na-doped sample. Finally, the atomic radius of K (2.27 Å) is larger than that of Na (1.54 Å), suggesting that a stronger charge transfer should occur between the *M* atoms and the Si cages in $K_xBa_ySi_{46}$. As a result, a higher concentration of electrons in antibonding band states of the Si network is anticipated in the $K_xBa_ySi_{46}$ clathrate, and one could expect to observe weakened Si-Si bonds and a concomitant downshift in the phonon mode frequencies. Clearly, better theoretical calculations are needed to identify which of these physical processes are the most important, or if some other mechanism is responsible.

Another intriguing difference in the room-temperature Raman spectra of the superconducting clathrates is the increased linewidths observed for several lines in the $Na_{0.2}Ba_{5.6}Si_{46}$ spectrum over their counterparts in $K_{2.9}Ba_{4.9}Si_{46}$ (see Table III). In general, the linewidth of a Raman-active phonon band is inversely proportional to the phonon lifetime. Two intrinsic contributions to the phonon lifetime are normally important: an anharmonic interaction (or phonon-phonon scattering), and the electron-phonon interaction (or electron-phonon scattering). The latter is more important in metals than semiconductors, as significantly more free electrons are available to scatter phonons in a metal. The Raman linewidth broadening contribution ($\Delta\Gamma$) due to the electron-phonon interaction can be related to the electron-phonon coupling constant λ via[24]

$$\lambda = \sum_i \lambda_i = \sum_i C \frac{\Delta\Gamma_i}{\omega_i^2}\left[\frac{1}{N(\varepsilon_F)}\right], \qquad (2)$$

where ω_i is the unrenormalized discrete phonon frequency for the ith phonon mode, $C_i = d_i/\pi$, and d_i is the degeneracy of the ith mode. According to Eq. (2), the Raman line broadening observed in the $Na_{0.2}Ba_{5.6}Si_{46}$ sample might be attributed to an increased electron-phonon coupling that decreases the phonon lifetime and increases the Raman linewidths. However, two factors argue against this interpretation for the linebroadening: (1) since the T_c's of these two materials are comparable, it is difficult to make a convincing argument for enhanced electron-phonon coupling in one clathrate sample over the other, (2) comparable Raman linewidths are observed in the nonsuperconducting Na_8Si_{46} and K_7Si_{46} samples [Fig. 2(b)]. We feel that an extrinsic mechanism, such as doping disorder must also play an important role in the line broadening. Ideally, we should determine the Raman linewidths for the semiconducting, empty cage Si_{46} clathrate, calculate the line broadening $\Delta\Gamma_i$ [Eq. (2)] for all the modes, and compare $\lambda N(\varepsilon_F)$ for the superconducting samples with that for the metallic samples. Practically speaking, Raman data for the empty cage Si_{46} are not available, and furthermore we have not observed all the twenty modes predicted by group theory. So this comparison cannot be made. Furthermore, we cannot separate the electron-phonon contribution to $\Delta\Gamma_i$ from that due to an extrinsic mechanism, such as doping disorder. This materials problem also precludes an experimental determination for $\lambda N(\varepsilon_F)$ in all samples, except for the Na_8Si_{46} sample that should not exhibit doping disorder.

Extrinsic mechanisms also can broaden the Raman lines, and should be considered. One such mechanism is disorder-induced broadening. In this case, the disorder breaks down the Γ-point phonon ($q \approx 0$) selection rule (i.e., that only zero wave vector phonons participate in the first-order scattering). In this case, other phonons with small, but nonzero q vector and slightly different frequency may also contribute to the Raman line, thereby inducing line broadening. In the samples considered here, x-ray-diffraction data reveal no significant difference in the diffraction peak width, suggesting that both samples exhibit more or less the same crystalline order. However, the Raman-scattering probe may indeed be more sensitive than x-ray diffraction to disorder in these clathrates, particularly if the disorder in the clathrate system is simply a random occupation of the cages with dopant species rather than, for example, broken bonds or missing atoms in the Si cage structure. In other words, although the Si superstructure can be in reasonably good order, a significant number of the Si_{20} cages may be missing an alkali metal (*M*) atom (or ion), and/or, significant doping of the larger Si_{24} cages by *M* atoms (ions) may also occur. Furthermore, several experiments,[4,19,25,26] including recent NMR studies,[27] suggest that not all the Na in $Na_xBa_ySi_{46}$ is ionized. This implies that Na may be present in both the neutral Na^0 and charged Na^+ forms. Because of charge transfer to the Si structure, these two valence possibilities also introduce a disorder-induced line broadening as well, i.e., charge-transfer disorder. This random doping of the Si cages might be expected to induce considerable local strain in the Si superstructure, leading to a disorder-induced, line broadening of predominantly Si-displacement phonon modes. Along these lines, it should be remembered that a significant doping difference occurs in the two superconducting clathrate samples studied here. The measured sample stoichiometries ($Na_{0.2}Ba_{5.6}Si_{46}$, $K_{2.9}Ba_{4.9}Si_{46}$) indicate that the Na-doped sample should have only one tenth of the small cages (Si_{20}) filled by *M* atoms, as compared to a fully occupied set of Si_{20} cages in the K-doped sample. Furthermore, as the K-doped sample has 2.9 K atoms per formula unit, presumably, the excess 0.9 K ions per formula unit reside in the larger Si_{24} cages in competition with the Ba dopant. The Na-doped Ba-clathrate sample is expected to exhibit stronger doping disorder via incomplete filling of the Si_{20} cages, whereas this disorder should be all but missing in the K-doped sample. On this basis, one would expect broader lines in the Na-doped Ba clathrate, as observed here. The observed line broadening in the Na-doped Ba clathrate may be due to doping disorder

in the smaller Si_{20} cages rather than to electron-phonon coupling. This line of reasoning can be applied to the metallic line compounds Na_8Si_{46} and K_7Si_{46}. In Na_8Si_{46}, all the cages are full, and we therefore expect the electron-phonon and phonon-phonon broadening mechanisms to be dominant. However, in K_7Si_{46}, one out of eight cages is empty. Therefore, in addition to these two intrinsic broadening mechanisms, we anticipate a third important extrinsic, disorder-induced mechanism in K_7Si_{46}. This proposal is consistent with the spectra shown in Fig. 2(b), where the Raman linewidths in the Na_8Si_{46} spectrum are, overall, noticeably narrower than in the K_7Si_{46} spectrum.

Futhermore, increasing the *M* concentration in the lattice increases the free electron concentration and increases the electron-phonon scattering rate. The charge transfer from alkali-metal atoms to Si cages in the Si_{46} clathrate system is supported by theoretical calculations,[18] NMR data on $Na_xBa_ySi_{46}$ sample,[25] and electron paramagnetic resonance studies on the related M_xSi_{136} clathrate system.[19,26] Thus, for the Na-doped Ba-clathrate sample, which chemical analysis indicates has considerably less *M* dopant, we anticipate a lower conduction electron concentration than in the K-doped Ba-clathrate sample, and therefore narrower Raman lines should be observed. This prediction is contrary to what is observed here, and so it appears we can rule out the electron-phonon interaction as the largest line broadening contribution.

In order to see the contribution of the phonon-phonon interaction in the Raman line broadening in Si clathrates, we measured Raman spectrum of $K_{2.9}Ba_{4.9}Si_{46}$ at 10 K (Fig. 3). Most of the frequencies upshift with decreasing temperature as expected for a simple lattice contraction on cooling. It is found that most of the modes observed at 10 K are narrower compared to those observed at 300 K, indicating that phonon-phonon interaction is an another important factor for the Raman line broadening at room temperature. The frequencies and linewidths for the 10 K spectrum are also tabulated in Table III.

CONCLUSIONS

Fifteen of the eighteen Si related first-order Raman frequencies for a Si_{46} clathrate have been detected. Normal-state Raman-scattering data on the superconducting $M_xBa_ySi_{46}$ system do not appear to support an enhanced electron-phonon coupling constant in these materials over

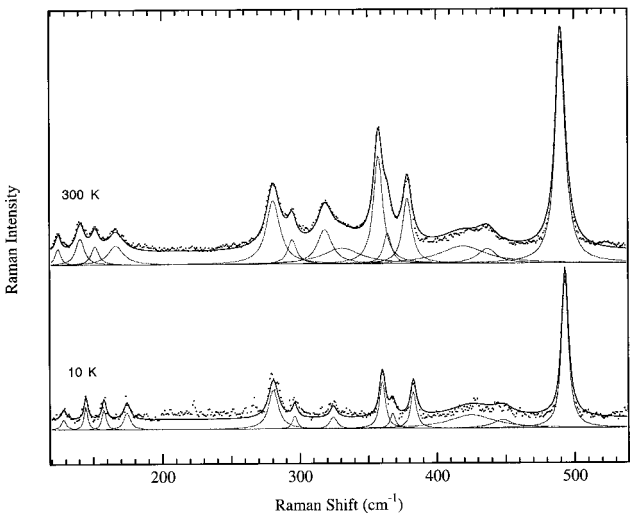

FIG. 3. Raman spectra of $K_{2.9}Ba_{4.9}Si_{46}$ at $T=300$ K (top) and $T=10$ K (bottom). The data are represented by the points and the solid line is the fit to the spectrum.

that of the Na_8Si_{46} and K_7Si_{46} materials that are not superconducting (at least down to 2 K). The most important line broadening mechanism in the Ba-containing clathrate appears to be due to doping disorder in the Si_{20} cages. Our data cannot explain why superconductivity is observed at $\sim$3.5 K in the $M_xBa_ySi_{46}$ materials, but not observed in Na_8Si_{46} and K_7Si_{46}.

Many of the mode frequencies in the $K_{2.9}Ba_{4.9}Si_{46}$ sample were found to be downshifted relative to their counterparts in the $Na_{0.2}Ba_{5.6}Si_{46}$ sample. Various mechanisms for this have been proposed. Further theoretical calculations on the phonon modes in these materials are needed to understand the doping-induced effects observed in this study.

ACKNOWLEDGMENTS

This work was supported in part by Grants from APRA Contract No. MDA 972-95-1-0021 (S.L.F. and P.C.E.) and NSF EPSCOR Contract No. OSR 9452895 (L.G.), and NSF DMR No. 9510093 (G.D. and M.S.D.). This study has been supported by CREST (Core Research for Evolutional Science and Technoloty) of Japan Science and Technology Corporation (JST) and Grant-in-Aid for Scientific Research on Priority Areas (No. 09239236) from Ministry of Education, Science, Sports and Culture, Japan.

[1] H. Kawaji, H. Horie, S. Yamanaka, and M. Ishikawa, Phys. Rev. Lett. **74**, 1427 (1995).

[2] S. Yamanaka, H. O. Horie, H. Kawaji, and M. Ishikawa, Eur. J. Solid State Inorg. Chem. **32**, 799 (1995).

[3] J. S. Kasper, P. Hagenmuller, M. Pouchard, and C. Cros, Science **150**, 1713 (1965).

[4] C. Cros, M. Pouchard, and P. J. Hagenmuller, Solid State Chem. **2**, 570 (1970).

[5] *Zeolite Chemistry and Catalysis*, edited by J. A. Rabo (American Chemical Society, Washington, 1976).

[6] K. A. Kvenvolden, Organic Geochem. **23**, 997 (1995).

[7] M. S. Dresselhaus, G. Dresselhaus, and P. C. Eklund, *Science of Fullerenes and Carbon Nanotubes* (Academic, New York, 1996).

[8] Q. Zhou, O. Zhou, N. Coustel, G. B. M. Vanghan, J. P. McCauley, Jr., W. J. Romanow, J. E. Fisher, and A. B. Smith III, Science **254**, 545 (1991).

[9] K. Holczer, O. Klein, G. Gruner, J. D. Thompson, F. Diederich, and R. L. Whetten, Phys. Rev. Lett. **67**, 271 (1991).

[10] G. B. Adams, M. O'Keefe, A. A. Demkov, O. F. Sankey, and Y. M. Huang, Phys. Rev. B **49**, 8048 (1994).

[11] A. G. Cullis and L. T. Canham, Nature (London) **353**, 335 (1991).

[12] L. Grigorian, S. L. Fang, and P. C. Eklund (unpublished).
[13] A. A. Demkov, O. F. Sankey, K. E. Schmidt, G. B. Adams, and M. O'Keefe, Phys. Rev. B **50**, 17 001 (1994).
[14] D. Kan and J. Lu, Phys. Rev. B **56**, 13 898 (1997).
[15] R. Alben, D. Weaire, J. E. Smith, Jr., and M. H. Brodsky, Phys. Rev. B **11**, 2271 (1975).
[16] M. Menon, E. Richter, K. R. Subbaswamy, Phys. Rev. B **56**, 12 290 (1997).
[17] S. Yamanaka, H. O. Horie, H. Nakano, and M. Ishikawa, Fullerene Sci. Technol. **3**, 21 (1995).
[18] S. Saito and S. Oshiyama, Phys. Rev. B **51**, 2628 (1995).
[19] S. B. Roy, K. E. Sim, and A. D. Caplin, Philos. Mag. B **65**, 1445 (1992).
[20] *International Tables for Crystallography*, edited by T. Hahn (Reidel, Dordrecht, 1983), Vol. A, p, 671.
[21] W. G. Fateley, F. R. Dollish, N. T. McDevitt, and F. F. Bentley, *Infrared and Raman Selection Rules for Molecular and Lattice Vibrations: the Correlation Method* (Wiley-Interscience, New York, 1972).
[22] H. Nakano and S. Yamanka, J. Solid State Chem. **108**, 260 (1994).
[23] S. L. Fang, L. Grigorian, and P. C. Eklund (unpublished).
[24] P. Zhou, K.-A. Wang, P. C. Eklund, G. Dresselhaus, and M. S. Dresselhaus, Phys. Rev. B **48**, 8412 (1993).
[25] J. Gryko, P. F. McMillan, and O. F. Sankey, Phys. Rev. B **54**, 3037 (1996).
[26] H. Yashiro, K. Yamaji, M. Shiotani, S. Yamanaka, and M. Ishikawa, Chem. Phys. Lett. **246**, 167 (1995).
[27] F. Shimizu, Y. Maniwa, K. Kume, H. Kawaji, S. Yamanaka, and M. Ishikawa, Phys. Rev. B **54**, 13 242 (1996).